New Rate Constants for D + H_2 and H + D_2 Between ∼1150 and 2100 K

J. V. Michael,* M.-C. Su,† and J. W. Sutherland‡

Chemistry Division, Argonne National Laboratory, Argonne, Illinois 60439

Received: July 14, 2003; In Final Form: September 26, 2003

The shock tube technique with D- and H-atom atomic resonance absorption spectrometric (ARAS) detection has been used to measure rate constants for two isotopic modifications of the most fundamental chemical reaction, H + H_2 → H_2 + H: D + H_2 → HD + H (1) and H + D_2 → HD + D (2). Hydrogen atoms were produced from the thermal decomposition of either C_2D_5I or C_2H_5I. Ethyl iodide decomposition above ∼1150 K is fast, and the product ethyl radicals decompose even faster, giving ethylene and hydrogen atoms. This clean source of atoms then allows for first-order analysis of both reactant and product hydrogen atoms for determining rate constants. The rate constant results can be described by the Arrhenius expressions $k_1 = 3.17 \times 10^{-10} \exp(-5207K/T)$ cm^3 molecule^{-1} s^{-1}, over the temperature range 1166−2112 K, and $k_2 = 2.67 \times 10^{-10} \exp(-5945K/T)$ cm^3 molecule^{-1} s^{-1}, over the temperature range 1132−2082 K. These new results are compared to earlier results and supply additional values for evaluating the rate behavior for both reactions over the very large temperature range ∼200−2200 K. These evaluations are then compared to recent quantum mechanical scattering calculations of the thermal rate behavior that are based on a new and quite accurate potential energy surface (i.e., globally accurate to ∼0.01 kcal mol^{-1}). Within experimental error, there is now complete convergence between the experimental evaluation and the new theory, bringing to completion a 75-year effort in chemical kinetics and dynamics. This is the first completely solved problem in chemical kinetics.

Introduction

For historical reasons, the reaction H + H_2 → H_2 + H is the most important chemical reaction in gas-phase chemical kinetics. Starting about 75 years ago with the work of London, Pelzer, and Wigner, Wynne-Jones and Eyring, and Evans and Polanyi,[1] the theoretical strategy of how to estimate thermal rate constants for gas-phase chemical reactions was outlined. The potential energy of interaction must first be known, and then a method for estimating the dynamics must be applied. About 60 years ago a semiempirical potential energy surface (PES) had been identified, and the temperature dependence of thermal rate constants was estimated for the H + H_2 reaction[2,3] using classical transition-state theory (CTST). It should be noted that CTST was originally developed for these calculations. Limited experimental data were also available for comparison to theory.[3,4]

As computational power has increased, the theoretical prediction of the ab initio PES for the H + H_2 reaction has undergone numerous iterations[5−10] from the original semiempirical estimates. By 1980, the best available PES (the Liu−Siegbahn−Truhlar−Horowitz (LSTH) fit of earlier ab initio electronic structure results[5]) was used with variational transition-state theory (VTST) to predict the thermal rate behavior.[11] Full-dimensional approximate quantum scattering calculations were presented for both D + H_2 and H + D_2 using the LSTH PES.[12] A newer PES fitting procedure, the double many-body expansion (DMBE) fit,[6] was then used with a reduced dimensionality dynamical method (the collinear exact quantum bend or CEQB), to calculate cumulative reaction probabilities that were then averaged over a Boltzmann distribution of reactants, giving estimates of thermal rate constants.[13] This was followed by full dimensional quantum scattering calculations using, among others, this new DMBE fit.[14] As has been pointed out by one of the authors,[15] the agreement between experiment and these early theoretical calculations is good, though not perfect.

In recent years, investigations of the PES have continued unabated,[7−10] resulting in a new and even more complete representation, the CCI potential energy surface, which is globally accurate to within ∼0.01 kcal mol^{-1}, and the differences between this new and earlier determinations have already been discussed.[10] The H + H_2 PES is now known with higher accuracy than PESs for all other chemical reactions. During the past 12 years, experimental design has also improved. Hence, thermal rate constants can now be measured at high temperatures with higher accuracy. These two new developments provide the motivation for the present investigation.

Rate constants for two isotopically substituted modifications of the H + H_2 reaction,

$$D + H_2 \rightarrow HD + H \quad (1)$$

and

$$H + D_2 \rightarrow HD + D \quad (2)$$

have been measured using the thermal dissociations of C_2D_5I as the source of D-atoms or C_2H_5I as the source for H-atoms. For both reactions, atomic depletion and formation experiments were performed under large excesses of H_2 or D_2, and therefore, the experiments were carried out under essentially pseudo-first-order conditions.

* Corresponding author. Address: D-193, Bldg. 200 Argonne National Laboratory Argonne, IL 60439. Phone: (630) 252-3171. Fax: (630) 252-4470. E-mail: jmichael@anl.gov.

† Faculty Research Participant, Department of Educational Programs, Argonne. Permanent address: Department of Chemistry, Butler University, Indianapolis, IN 46208.

‡ Present address: Guest Scientist, Energy Sciences and Technology Department, Brookhaven National Laboratory, Upton, NY 11973.

10.1021/jp030848k CCC: $27.50
Published on Web 12/19/2003

Experimental Section

The present experiments were performed with the shock tube technique using atomic resonance absorption spectrometric (ARAS) detection. The method and the apparatus currently being used have been previously described.[16,17] Therefore, only a brief description of the experiment will be presented here.

The apparatus consists of a 7-m (4-in.-o.d.) 304 stainless steel tube separated from the He driver chamber by a 4-mil unscored 1100-H18 aluminum diaphragm. The tube was routinely pumped between experiments to $<10^{-8}$ Torr by an Edwards Vacuum Products Model CR100P packaged pumping system. The velocity of the shock wave was measured with eight equally spaced pressure transducers (PCB Piezotronics, Inc., Model 113A21) mounted along the end portion of the shock tube, and the temperature and density in the reflected shock wave regime were calculated from this velocity and include corrections for boundary layer perturbations.[18−20] A 4094C Nicolet digital oscilloscope, triggered by delayed pulses that derive from the last velocity gauge signal, was used to record both the wave velocities and kinetics profiles.

H- and D-atom atomic resonance absorption spectrometric (ARAS) detection was used to follow $[H]_t$ and $[D]_t$ quantitatively, as described previously.[21−23] Adding small amounts of D_2 to the resonance lamp gave measurable Lyman-αD. Because the separation between H- and D-Lyman-α lines is substantial,[23] the D-line was isolated by using an H-atom atomic filter (a slowly flowing H_2 discharge flow system) between the resonance lamp and the shock tube window in the kinetics experiments.[24] This was necessary because Lyman-αH is still present in the unfiltered lamp. The entire photometer system was radially located at the distance of 6 cm from the end plate. MgF_2 components were used in the photometer optics. The resonance lamp beam was detected by an EMR G14 solar blind photomultiplier tube, and the resultant time profile of ARAS signals was recorded with the oscilloscope.

High-purity He (99.995%), used as the driver gas, was from AGA Gases. Scientific grade Kr (99.999%), the diluent gas in reactant mixtures, was from Spectra Gases, Inc. The ∼10 ppm impurities (N_2 2 ppm, O_2 0.5 ppm, Ar 2 ppm, CO_2 0.5 ppm, H_2 0.5 ppm, CH_4 0.5 ppm, H_2O 0.5 ppm, Xe 5 ppm, and CF_4 0.5 ppm) are all either inert or in sufficiently low concentration so as to not perturb H- or D-atom profiles. Ultrahigh-purity grade He (99.999%) for the resonance lamp and high-purity H_2 (99.995%) for the atomic filter were from AGA Gases. Research grade D_2 (99.99%) from Air Products and Chemicals, Inc. was used in the resonance lamp and also in the experimental mixture preparation. Research grade H_2 (99.9999%) from MG Industries, was used in mixture preparation as received. Analytical grade C_2H_5I (99%) and C_2D_5I (99%), both from Aldrich Chemical Co. Inc., were purified by bulb-to-bulb distillation, retaining only the middle thirds. Test gas mixtures were accurately prepared from pressure measurements using a Baratron capacitance manometer and were stored in an all glass vacuum line.

Results

Rate constants for both reactions have been measured with the reflected shock tube technique[16,17] over the approximate temperature range ∼1150−2100 K. The D- or H-atoms, formed from the thermal decompositions of ethyl-d_5 iodide or ethyl iodide, are monitored by the ARAS technique. In earlier studies, rate constants and branching ratios for the thermal dissociations of both C_2D_5I[25] and C_2H_5I[26] were determined. In both cases, absolute atomic concentration profiles were measured, and from a knowledge of initial ethyl iodide concentrations, the atomic yields could be determined. From initial rates, the overall decomposition rate constants were likewise determined, giving atomic yields and rate constant ratios for the two decomposition processes, (1) ethyl radicals + I-atoms and (2) ethylene + hydrogen iodide. Due to the relatively low C−I bond strength, these decompositions are fast above ∼1150 K. The ethyl radicals produced in (1) subsequently decompose even faster, giving ethylene and hydrogen atoms. It is this overall process that gives a convenient and clean method for producing small atomic hydrogen concentrations for kinetics studies of the title reactions.

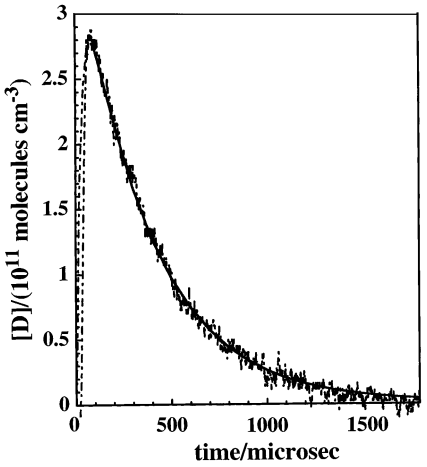

Figure 1. D-atom profile plot for an experiment at $P_1 = 10.89$ Torr and $M_s = 2.272$. $T_5 = 1317$ K, $[C_2D_5I] = 5.157 \times 10^{11}$ molecules cm^{-3}, and $[H_2] = 4.657 \times 10^{14}$ molecules cm^{-3}. The solid line is a simulation using a 35-step mechanism (see text).

Figure 1 shows a typical profile for the D + H_2 reaction. From known $[C_2D_5I]_0$, this experiment can be modeled with a 35 step mechanism including reaction 1 (and/or (2)), and the predicted profile (solid line in Figure 1) is determined only by rate constants for C_2D_5I thermal dissociation, which is fixed, and reaction 1, which is fitted. Modeling shows that $[C_2D_5I]$ becomes negligible after ∼200 μs, and therefore, the atoms should decay at long times with a pseudo-first-order rate law. The fitted value from the full mechanism should be the same as that recovered by the first-order analysis.

First-order analysis is straightforward because the level of resonance light absorption is small and Beer's law is obeyed. Hence, the atomic concentration is equal to (ABS)/σl where (ABS) is $-\ln T$, σ is the effective absorption cross section, and l is the absorption path length. T is the ratio of the temporally transmitted to initial intensities of the resonance radiation. The rate of atom removal in reaction 1 (or (2)), $R = -d[D]/dt$ (or $-d[H]/dt$) is $k_1[H_2][D]$ (or $k_2[D_2][H]$). Because little reactant is consumed, the concentration of H_2 (or D_2) can be taken to be constant in time. The atomic concentration then follows a first-order rate law with the first-order decay constant, k_{first}, being equal to $k_1[H_2]$ (or $k_2[D_2]$); thus, $\ln[D]_t$ (or $\ln[H]_t$) $= -k_{first}t +$ const. Because the atomic concentration is proportional to (ABS), the first-order decay constant can be obtained simply by plotting $\ln[(ABS)_t]$ as a function of time and calculating the negative slope, and the bimolecular rate constants are determined by dividing k_{first} by $[H_2]$ (or $[D_2]$). Figure 2 shows the first-order plot corresponding to the profile shown in Figure 1. The bimolecular rate constant recovered from the first-order analysis is identical to that obtained from the full model.

Rate constants can also be determined by observing product atoms in reactions 1 and 2, i.e., H in D + H_2 and D in H + D_2. First-order analysis at long times gives the rate law, $\ln\{([H]_\infty$

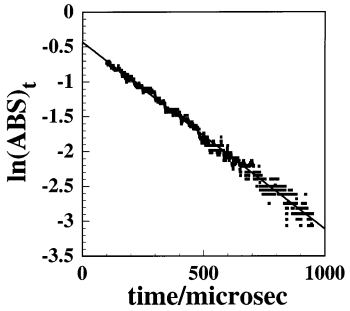

Figure 2. First-order D-atom decay plot for the experiment shown in Figure 1. $k_{first} = 2698 \pm 23$ s^{-1}. The corresponding second-order rate constant is 5.79×10^{-12} cm^3 molecule^{-1} s^{-1} and is identical to the value used in the simulation shown in Figure 1.

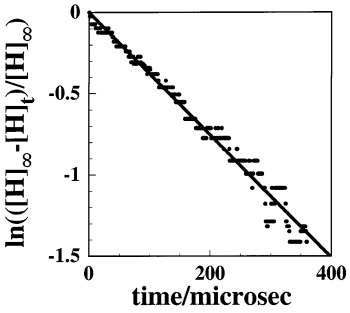

Figure 3. First-order H-atom formation plot for a typical D + H_2 experiment with $P_1 = 10.93$ Torr and $M_s = 2.279$. $T_5 = 1324$ K, $[C_2D_5I] = 5.193 \times 10^{11}$ molecules cm^{-3}, and $[H_2] = 4.689 \times 10^{14}$ molecules cm^{-3}. $k_{first} = 3665 \pm 159$ s^{-1}. The corresponding second-order rate constant is 7.82×10^{-12} cm^3 molecule^{-1} s^{-1}.

$- [H]_t)/[H]_\infty\} = -k_{first}t$ (or $\ln\{([D]_\infty - [D]_t)/[D]_\infty\} = -k_{first}t$). Figure 3 shows an example of this analysis for the D + H_2 reaction.

The experimental conditions and rate constants obtained from both types of experiments for both reactions are given in Tables 1 and 2. Arrhenius plots are shown in Figures 4 and 5 along with linear-least-squares lines determined from these data. Over the temperature range 1166−2112 K, the data for reaction 1 can be expressed as

$$k_1 = 3.17 \times 10^{-10} \exp(-5207K/T) \text{ cm}^3 \text{ molecule}^{-1} \text{ s}^{-1} \quad (3)$$

with a one standard deviation of the points from the line of ±11%. The results for reaction 2 are

$$k_2 = 2.67 \times 10^{-10} \exp(-5945K/T) \text{ cm}^3 \text{ molecule}^{-1} \text{ s}^{-1} \quad (4)$$

for the temperature range 1132−2082 K. The points exhibit a ±12% one standard deviation error from the line.

Discussion

The present results can be compared to earlier shock tube results from this laboratory.[27,28] The earlier data were obtained using the flash photolysis-shock tube (FP-ST) technique with D_2O and H_2O (or NH_3) as photolytic sources in the two studies. The Arrhenius expressions, applicable temperature ranges, and one standard deviations of the data from the expressions, are given in Table 3. For both reactions, the present data are ∼25% lower than the earlier results; however, it is gratifying to note that the present and earlier sets easily overlap within combined one standard deviations over mutual temperature ranges. We note that the earlier FP−ST results had to be corrected by subtracting the contributions due to atom plus photolytic precursor from the observed first-order decay constants. This contribution is negligible at ∼700 K but becomes more important at temperatures above ∼1400 K. Such complications are negligible in the present case even though the present thermal dissociation method for preparing atoms limits the temperature range over which data can be obtained, i.e., greater than 1150 K.

TABLE 1: High-Temperature Rate Data for D + H_2 → H + HD

P_1/Torr	M_s[a]	$\rho_5/(10^{18}$ cm$^{-3})$[b]	T_5/K[b]	k_{first}/s^{-1}	$k_1/$(cm^3 s^{-1})[c]
		D-Atom ARAS			
		$X_{C_2D_5I} = 2.985 \times 10^{-7}$, $X_{H_2} = 2.063 \times 10^{-4}$			
5.96	2.724	1.226	1846	3854	1.52(−11)[d]
5.92	2.813	1.243	1959	5601	2.18(−11)
5.93	2.850	1.258	2006	5925	2.28(−11)
5.95	2.922	1.287	2102	7750	2.91(−11)
5.95	2.622	1.176	1721	3432	1.41(−11)
5.95	2.363	1.064	1426	1698	7.74(−12)
5.97	2.381	1.075	1445	1782	8.03(−12)
5.93	2.246	1.004	1303	944	4.56(−12)
10.91	2.607	2.131	1694	5986	1.36(−11)
10.90	2.652	2.162	1747	6838	1.53(−11)
10.92	2.866	2.312	2016	11298	2.37(−11)
10.90	2.761	2.239	1882	9194	1.99(−11)
10.98	2.472	2.039	1537	3593	8.54(−12)
10.97	2.538	2.090	1613	5433	1.26(−11)
10.90	2.333	1.908	1385	2601	6.60(−12)
10.92	2.253	1.840	1301	2123	5.59(−12)
10.91	2.303	1.877	1357	3016	7.79(−12)
		$X_{C_2D_5I} = 2.774 \times 10^{-7}$, $X_{H_2} = 2.505 \times 10^{-4}$			
10.98	2.369	1.973	1409	3794	7.68(−12)
10.90	2.397	1.976	1444	4285	8.66(−12)
10.91	2.520	2.086	1576	5739	1.10(−11)
10.92	2.712	2.224	1808	8410	1.51(−11)
10.88	2.807	2.289	1922	13455	2.35(−11)
10.86	2.131	1.728	1171	1769	4.11(−12)
10.97	2.260	1.868	1300	3008	6.21(−12)
10.89	2.272	1.859	1317	2698	5.79(−12)
10.91	2.130	1.741	1166	1787	4.10(−12)
5.94	2.690	1.209	1792	6179	2.04(−11)
5.92	2.769	1.235	1891	5992	1.94(−11)
5.94	2.820	1.258	1955	7407	2.35(−11)
5.95	2.819	1.256	1960	7098	2.26(−11)
5.98	2.939	1.309	2112	9444	2.88(−11)
5.96	2.573	1.166	1652	4337	1.49(−11)
5.95	2.437	1.101	1502	3156	1.14(−11)
		$X_{C_2D_5I} = 3.136 \times 10^{-7}$, $X_{H_2} = 5.206 \times 10^{-4}$			
10.92	2.198	1.802	1237	4542	4.84(−12)
10.97	2.187	1.799	1226	4052	4.33(−12)
10.94	2.142	1.751	1181	3005	3.30(−12)
10.94	2.199	1.799	1241	4297	4.59(−12)
10.88	2.229	1.817	1272	4734	5.00(−12)
10.94	2.178	1.785	1217	3840	4.13(−12)
		H-Atom ARAS			
		$X_{C_2D_5I} = 2.774 \times 10^{-7}$, $X_{H_2} = 2.505 \times 10^{-4}$			
10.94	2.486	2.050	1547	5966	1.16(−11)
10.96	2.317	1.911	1363	3463	7.24(−12)
10.98	2.429	2.018	1479	4730	9.36(−12)
10.98	2.321	1.918	1367	3416	7.11(−12)
10.89	2.317	1.899	1363	3895	8.19(−12)
10.94	2.255	1.851	1298	2911	6.28(−12)
10.93	2.279	1.872	1324	3665	7.82(−12)
10.98	2.282	1.890	1322	3071	6.49(−12)
5.97	2.444	1.112	1505	3492	1.25(−11)
5.95	2.365	1.072	1418	1904	7.09(−12)
5.93	2.696	1.210	1799	5818	1.92(−11)

[a] The error in measuring the Mach number, M_s, is typically 0.5−1.0% at the one standard deviation level. [b] Quantities with the subscript 5 refer to the thermodynamic state of the gas in the reflected shock region. [c] Rate constants for reaction 1 using first-order analysis as described in the text. [d] Parentheses denotes the power of 10.

TABLE 2: High-Temperature Rate Data for H + D_2 → D + HD

P_1/Torr	M_s[a]	ρ_5/(10^{18} cm^{-3})[b]	T_5/K[b]	k_{first}/s^{-1}	k_2/(cm^3 s^{-1})[c]
H-Atom ARAS					
$X_{C_2H_5I} = 8.591 \times 10^{-7}$, $X_{D_2} = 4.678 \times 10^{-4}$					
5.94	2.888	1.282	2042	11369	1.90(−11)[d]
5.91	2.742	1.223	1856	6749	1.18(−11)
5.97	2.592	1.176	1674	4508	8.20(−12)
5.96	2.388	1.081	1449	2436	4.82(−12)
5.94	2.460	1.110	1528	3035	5.85(−12)
5.95	2.653	1.197	1747	4420	7.90(−12)
5.94	2.715	1.210	1834	5442	9.61(−12)
5.96	2.814	1.260	1947	7777	1.32(−11)
5.96	2.918	1.297	2082	10066	1.66(−11)
5.96	2.767	1.234	1900	8282	1.43(−11)
10.96	2.621	2.151	1710	7792	7.74(−12)
10.94	2.431	2.005	1486	5250	5.60(−12)
10.95	2.152	1.762	1191	1823	2.21(−12)
10.97	2.343	1.942	1386	3413	3.76(−12)
10.98	2.504	2.072	1568	6120	6.32(−12)
10.94	2.660	2.176	1757	8389	8.24(−12)
10.92	2.716	2.226	1813	10682	1.03(−11)
10.96	2.284	1.881	1328	2530	2.88(−12)
$X_{C_2H_5I} = 6.562 \times 10^{-7}$, $X_{D_2} = 5.439 \times 10^{-4}$					
5.94	2.364	1.062	1427	2396	4.15(−12)
5.98	2.497	1.129	1574	3421	5.57(−12)
5.96	2.440	1.101	1510	3005	5.02(−12)
5.97	2.303	1.046	1353	1624	2.86(−12)
5.95	2.225	1.000	1276	1286	2.36(−12)
5.95	2.296	1.039	1345	2173	3.85(−12)
10.97	2.350	1.935	1403	3537	3.36(−12)
10.95	2.243	1.848	1282	2553	2.54(−12)
10.95	2.090	1.701	1132	1141	1.23(−12)
10.94	2.145	1.754	1184	1553	1.63(−12)
10.97	2.304	1.894	1354	3378	3.28(−12)
10.94	2.330	1.919	1377	3492	3.35(−12)
10.93	2.487	2.056	1544	6205	5.55(−12)
D-Atom ARAS					
$X_{C_2H_5I} = 8.591 \times 10^{-7}$, $X_{D_2} = 4.678 \times 10^{-4}$					
5.97	2.565	1.157	1653	3946	7.29(−12)
5.94	2.558	1.156	1634	3140	5.81(−12)
5.94	2.482	1.123	1547	2783	5.30(−12)
$X_{C_2H_5I} = 6.562 \times 10^{-7}$, $X_{D_2} = 5.439 \times 10^{-4}$					
5.96	2.372	1.069	1435	2073	3.56(−12)
5.95	2.809	1.252	1947	9594	1.41(−11)
5.96	2.840	1.261	1993	8690	1.27(−11)
5.97	2.847	1.278	1983	9132	1.31(−11)
5.90	2.640	1.177	1737	5646	8.82(−12)
5.91	2.591	1.164	1673	3833	6.06(−12)
5.97	2.525	1.144	1602	3563	5.73(−12)
5.98	2.476	1.132	1535	3026	4.92(−12)
10.95	2.323	1.915	1370	4292	4.12(−12)
10.98	2.240	1.840	1280	2936	2.93(−12)
10.94	2.100	1.715	1137	1675	1.80(−12)
10.96	2.184	1.789	1227	2123	2.18(−12)
10.96	2.336	1.928	1383	3972	3.79(−12)
10.97	2.368	1.964	1413	3801	3.56(−12)

[a] The error in measuring the Mach number, M_s, is typically 0.5−1.0% at the one standard deviation level. [b] Quantities with the subscript 5 refer to the thermodynamic state of the gas in the reflected shock region. [c] Rate constants for reaction 2 using first-order analysis as described in the text. [d] Parentheses denotes the power of 10.

Johnston and others[2] have considered the earlier data; however, we will consider only the direct determinations. Also in Table 3, three additional direct studies each are listed for the two reactions that have been carried out at low temperatures using discharge flow techniques with either electron spin resonance or product HD formation as the detection method

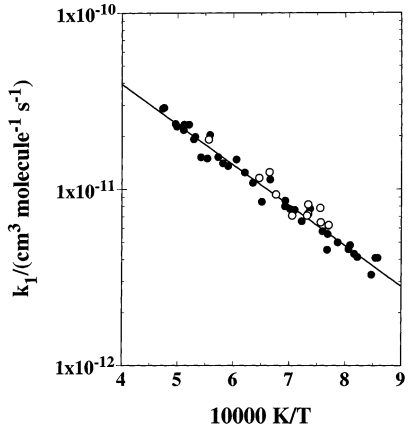

Figure 4. Arrhenius plot of shock tube data for D + H_2. The solid points are D-atom depletion experiments, and the open points are H-atom formation experiments. The solid line is a linear-least-squares fit to log k against T^{-1}, and the expression derived is eq 3.

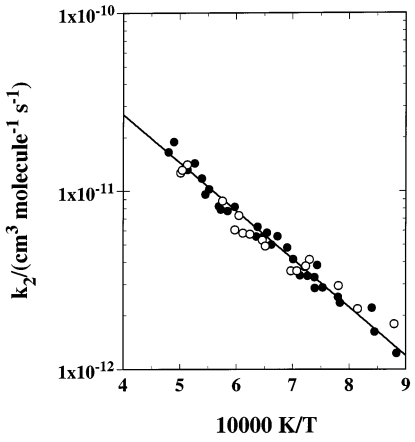

Figure 5. Arrhenius plot of shock tube data for H + D_2. The solid points are H-atom depletion experiments, and the open points are D-atom formation experiments. The solid line is a linear-least-squares fit to log k against T^{-1}, and the expression derived is eq 4.

TABLE 3: Earlier Least-Squares Experimental Rate Constant Expressions for D + H_2 and H + D_2[a]

ref	A/cm^3 molecule^{-1} s^{-1}	n	B/K	T range/K	one std dev %
D + H_2 → HD + H					
27	3.75(−10)[b]	0	4984	655−1979	±28
29	4.08(−11)	0	3628	274−468	±20
30	4.41(−11)	0	3560	252−745	±12
31	2.48(−25)	4.757	1870	167−346	±15
H + D_2 → HD + D					
28	3.95(−10)	0	5919	724−2160	±25
30	4.28(−11)	0	4362	299−745	±19
32	7.24(−12)	0	3671	368−468	±10[c]
33	2.12(−11)	0	4181	274−364	±11

[a] Rate constants are modified Arrhenius expressions, $k = AT^n \exp(-B/T)$. [b] Parentheses denote the power of 10. [c] Estimated, considering systematic and random errors.

for measuring rate constants.[29−33] All of the results in Table 3 have been combined with the present data described by eqs 3 and 4 to obtain an evaluation over the entire temperature range. For reasons given in the original references, we have eliminated the lowest T point from each of the three flow tube D + H_2 studies.[29−31] Including the present and the additional four sets in Table 3, each data set was given equal statistical weight but only over the temperature range of applicability for a given set. The data were then fitted to fifth-

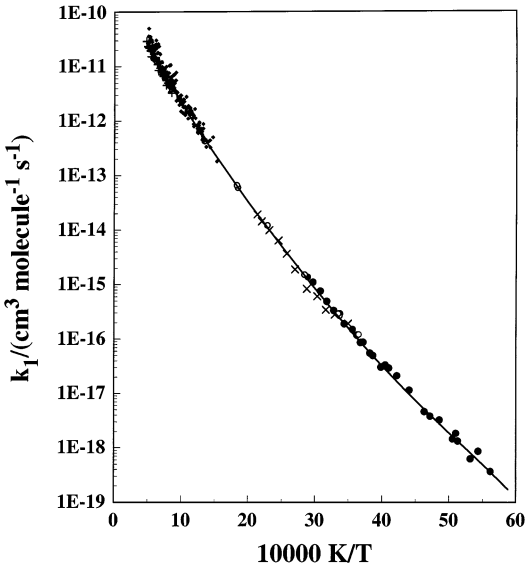

Figure 6. Arrhenius plot of experimental kinetics data for the D + H_2 reaction: (◆) ref 27; (×) ref 29; (○) ref 30; (●) ref 31; (+) present work. The solid line evaluation is a fifth-order least-squares polynomial fit to the data, eq 5, that is obtained by giving each set equal statistical weight.

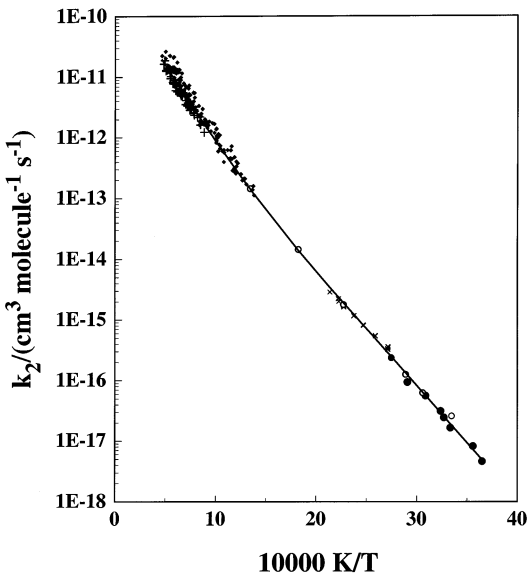

Figure 7. Arrhenius plot of experimental kinetics data for the H + D_2 reaction: (◆) ref 28; (×) ref 32; (○) ref 30; (●) ref 33; (+) present work. The solid line evaluation is a fifth-order least-squares polynomial fit to the data, eq 6, that is obtained by giving each set equal statistical weight.

order polynomials in log k against T^{-1}. The evaluated fit for the D + H_2 reaction is given by

$$\log k_1 = -1.778 \times 10^{12}/T^{-5} + 2.914 \times 10^{10}/T^{-4} - 1.844 \times 10^{8}/T^{-3} + 6.518 \times 10^{5}/T^{-2} - 2.864 \times 10^{3}/T - 9.300 \quad (5)$$

over the temperature range 167−2112 K. An Arrhenius plot of all the earlier and present experimental data is shown in Figure 6 along with the evaluation, eq 5. Similarly, the fit for the H + D_2 reaction is given by

$$\log k_2 = 1.451 \times 10^{13}/T^{-5} - 1.493 \times 10^{11}/T^{-4} + 5.172 \times 10^{8}/T^{-3} - 5.465 \times 10^{5}/T^{-2} - 2.335 \times 10^{3}/T - 9.557 \quad (6)$$

over the temperature range 274−2160 K, and Figure 7 shows eq 6 in comparison to all the data from which the equation was derived. For reactions 1 and 2, the individual data points (∼200 points in both cases) show one standard deviation of only ±32 and ±23%, respectively, from the polynomial fits, eqs 5 and 6, over the entire temperature ranges. Considering the variety of experimental methods and apparatuses, with attendant calibrations, the rate constant fits, which span nearly 9 orders of magnitude, are remarkably good over both very large temperature ranges.

New theoretical calculations have been carried out using the CCI PES,[10] with time independent quantum scattering[34] being the method for determining rate constants. These calculations have already been described,[35,36] and a new innovation is the consideration of specifically the diagonal correction to the Born−Oppenheimer (BO) approximation.[37] The dynamical calculations used the outgoing wave variational principle (OWVP) to calculate cumulative reaction probabilities for the CCI PES. Total angular momentum was taken into account, and converged BO results were obtained for both reactions 1 and 2. An approximate treatment of the diagonal correction was subsequently applied, and the final results were obtained.

The new theoretical results[35,36] can also be fitted to fifth-order polynomials in log k against T^{-1}. For D + H_2 from 170 to 2000 K,

$$\log k_1 = -2.043 \times 10^{12}/T^{-5} + 3.795 \times 10^{10}/T^{-4} - 2.624 \times 10^{8}/T^{-3} + 9.115 \times 10^{5}/T^{-2} - 3.161 \times 10^{3}/T - 9.242 \quad (7)$$

Equation 7 reproduces the theoretical values to within ±1.6% over the entire temperature range. A similar fit for H + D_2 between 200 and 2200 K is

$$\log k_2 = -3.775 \times 10^{12}/T^{-5} + 5.911 \times 10^{10}/T^{-4} - 3.561 \times 10^{8}/T^{-3} + 1.093 \times 10^{6}/T^{-2} - 3.674 \times 10^{3}/T - 9.181 \quad (8)$$

Equation 8 reproduces the theoretical values to within 0.7% over the temperature range.

The theoretical descriptions, eqs 7 and 8, can now be compared to the evaluations, eqs 5 and 6, respectively. All four equations are plotted in Figure 8 where the solid lines are evaluations and the dashed lines are theory. There is little difference between the corresponding equations. The new theoretical calculations agree well with experiment, particularly in the lower temperature region where previous predictions[13,14] were not as accurate. Over the entire temperature ranges, eq 5 differs from (7) by a one standard deviation value of ±9.4% whereas eq 6 differs from (8) by ±4.0%. Inspection of the present results, eqs 3 and 4, and also the data summarized in Table 3, shows that no data set for either reaction has smaller uncertainty than these values. We can claim that theory and experiment agree within experimental error. The consequence of this claim is that the theoretical values[35,36] should now be used to describe the rate behavior for these reactions. The convergence of experiment and theory is the completion of a 75 year old problem in chemical kinetics and dynamics.[1] It is therefore a very significant result and, as pointed out before,[35,36] ranks with earlier solved problems in molecular quantum mechanics, the short list which includes the electronic spectra

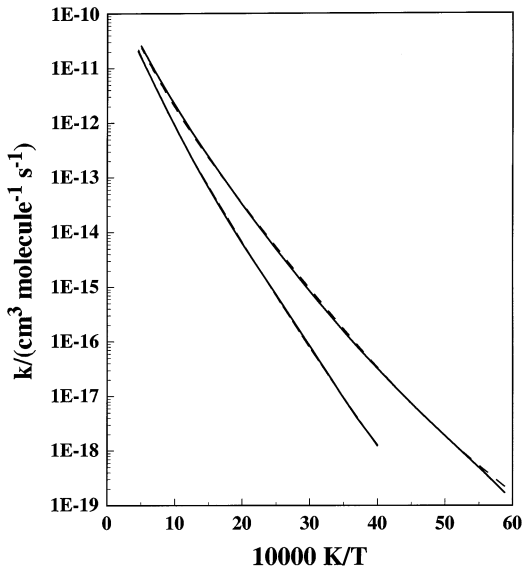

Figure 8. Arrhenius plots of experimental evaluations (eqs 5 and 6), —, and theoretical calculations (eqs 7 and 8), — — —, for the D + H_2 (top) and H + D_2 (bottom) reactions.

of H-[38] and He-atoms[39] and the vibrational−rotational spectra of H_2,[40] H_2^+,[41] and H_3^+.[42] The H + H_2 reaction can now be added to this list.

Acknowledgment. We thank S. L. Mielke, K. A. Peterson, D. W. Schwenke, B. C. Garrett, and D. G. Truhlar for prepublication theoretical results and for helpful discussions. This work was supported by the U. S. Department of Energy, Office of Basic Energy Sciences, Division of Chemical Sciences, under Contract No. W-31-109-Eng-38.

References and Notes

(1) London, F. *Probleme der Modernen Physik (Sommerfeld Festschrift*); 1928; p 104. London, F. *Z. Elektrochem.* **1929**, *35*, 552. Pelzer, H.; Wigner, E. *Z. Phys. Chem. B* **1932**, *58*, 445. Eyring, H. *J. Chem. Phys.* **1935**, *3*, 107. Wynne-Jones, W. F. K.; Eyring, H. *J. Chem. Phys.* **1935**, *3*, 492. Evans, M. G.; Polanyi, M. *Trans. Faraday Soc.* **1935**, *31*, 875. *Trans. Faraday Soc.* **1937**, *33*, 448. Polanyi, M. *J. Chem. Soc.*, **1937**, 62.

(2) For reviews of earlier theoretical and experimental work see: Glasstone, S.; Laidler, K. J.; Eyring, H. *The Theory of Rate Processes*; McGraw-Hill: New York, 1941. Laidler, K. J. *Chemical Kinetics*; McGraw-Hill: New York, l965. Johnston, H. S. *Gas-Phase Reaction Rate Theory*; Ronald: New York, 1966.

(3) Kaufman, F. *Annu. Rev. Phys. Chem.* **1969**, *20*, 43. Truhlar, D. G.; Wyatt, R. E. *Annu. Rev. Phys. Chem.* **1979**, *27*, 1.

(4) Truhlar. D. G.; Wyatt, R. E. *Adv. Chem. Phys.* **1977**, *36*, 141; see also ref 3 therein for a discussion of earlier semiempirical and ab initio calculations.

(5) Liu, B. *J. Chem. Phys.* **1973**, *58*, 1925. Siegbahn, P.; Liu, B. *J. Chem. Phys.* **1978**, *68*, 2457. Truhlar, D. G.; Horowitz, C. J. *J. Chem. Phys.* **1978**, *68*, 2466; **1979**, *71*, 1514E.

(6) Varandas, A. J. C.; Brown, F. B.; Mead, C. A.; Truhlar, D. G.; Blais, N. C. *J. Chem. Phys.* **1987**, *86*, 6258.

(7) Boothroyd, A. I.; Keogh, W. J.; Martin, P. G.; Peterson, M. R. *J. Chem. Phys.* **1991**, *95*, 4343. Boothroyd, A. I.; Keogh, W. J.; Martin, P. G.; Peterson, M. R. *J. Chem. Phys.* **1996**, *104*, 7139.

(8) Blomberg, M. R. A.; Liu, B. *J. Chem. Phys.* **1985**, *82*, 1050. Bauschlicher, C. W., Jr.; Langhoff, S. R.; Partridge, H. *Chem. Phys. Lett.* **1990**, *170*, 345; Partridge, H.; Bauschlicher, C. W., Jr.; Stallcop, J. R.; Levin, E. *J. Chem. Phys.* **1993**, *99*, 5951.

(9) Diedrich, D. L.; Anderson, J. B, *Science* **1992**, *258*, 786. Diedrich, D. L.; Anderson, J. B. *J. Chem. Phys.* **1994**, *100*, 8089.

(10) Mielke, S. L.; Garrett, B. C.; Peterson, K. A. *J. Chem. Phys.* **1999**, *111*, 3806; **2002**, *116*, 4142.

(11) Garrett, B. C.; Truhlar, D. G. *Proc. Natl. Acad. Sci. U.S.A.* **1979**, *76*, 4755. Garrett, B. C.; Truhlar, D. G. *J. Chem. Phys.* **1980**, *72*, 3460. Garrett, B. C.; Truhlar, D. G.; Varandas, A. J. C.; Blais, N. C. *Int. J. Chem. Kinet.* **1986,** *18*, 1065.

(12) Park, T. J.; Light, J. C. *J. Chem. Phys.* **1991**, *94*, 2946. Park, T. J.; Light, J. C. *J. Chem. Phys.* **1992**, *96*, 8853.

(13) Michael, J. V.; Fisher, J. R.; Bowman, J. M.; Sun, Q. *Science* **1990**, *249*, 269.

(14) Mielke, S. L.; Lynch, G. C.; Truhlar, D. G.; Schwenke, D. W. *J. Phys. Chem.* **1994**, *98*, 8000.

(15) Michael, J. V.; Lim, K. P. *Annu. Rev. Phys. Chem.* **1991**, *44*, 429. Michael, J. V. In *Gas-Phase Chemical Reaction Systems: Experiments and Models 100 Years after Max Bodenstein*; Wolfrum, J., Volpp, H.-R., Rannacher, R., Warnatz, J., Eds.; Springer-Verlag: Heidelberg, 1996; pp 177−189. Kumaran, S. S.; Michael, J. V. *J. Phys. Chem.* **1996**, *100*, 20172.

(16) Michael, J. V. *Prog. Energy Combust. Sci.* **1992**, *18*, 327.

(17) Michael, J. V. In *Advances in Chemical Kinetics and Dynamics*, Barker, J. R., Ed.; JAI: Greenwich, CT, 1992; Vol. I, pp 47−112 (for original references).

(18) Michael, J. V.; Sutherland, J. W. *Int. J. Chem. Kinet.* **1986**, *18*, 409.

(19) Michael, J. V. *J. Chem. Phys.* **1989**, *90*, 189.

(20) Michael, J. V.; Fisher J. R. In *Seventeenth International Symposium on Shock Waves and Shock Tubes*; Kim, K. W., Ed.; AIP Conference Proceedings 208; American Institute of Physics: New York, 1990; pp 210−215.

(21) Lim, K. P.; Michael, J. V. *Proc. Combust. Inst.* **1994**, *25*, 713 and references therein.

(22) Kumaran, S. S.; Su, M.-C.; Lim, K. P.; Michael, J. V. *Proc. Combust. Inst.* **1996**, *26*, 605.

(23) Michael, J. V.; Lifshitz, A. In *Handbook of Shock Waves*; Ben-Dor, G., Igra, O., Elperin, T., Lifshitz, A., Eds.; Academic Press: New York, 2001; Vol. 3, pp 77−105.

(24) Fisher, J. R.; Michael, J. V. *J. Phys. Chem.* **1990**, *94*, 2465.

(25) Su, M.-C.; Michael, J. V. *Proc. Combust. Inst.* **2002**, *29*, 1219.

(26) Herzler, J.; Frank, P. *Ber. Bunsen-Ges. Phys. Chem.* **1992**, *96*, 1333; Mertens, J. D.; Wooldridge, M. S.; Hanson, R. K. *Eastern States Section 1994 Technical Meeting*; The Combustion Institute: Pittsburgh, 1994; p 106. Kumaran, S. S.; Su, M.-C.; Lim, K. P.; Michael, J. V. *Proc. Combust. Inst.* **1996**, *26*, 605.

(27) Michael, J. V.; Fisher, J. R. *J. Phys. Chem.* **1990**, *94*, 3318.

(28) Michael, J. V. *J. Chem. Phys.* **1990**, *92*, 3394.

(29) Ridley, B. A.; Schulz, W. R.; Le Roy, D. J. *J. Chem. Phys.* **1966**, *44*, 3344.

(30) Westenberg, A. A.; de Haas, N. *J. Chem. Phys.* **1967**, *47*, 1393.

(31) Mitchell, D. N.; Le Roy, D. J. *J. Chem. Phys.* **1973**, *58*, 3449.

(32) Schulz, W. R.; Le Roy, D. J. *Can. J. Chem.* **1965**, *42*, 2480.

(33) Jayaweera, I. S.; Pacey, P. D. *J. Phys. Chem.* **1990**, *94*, 3614.

(34) Mielke, S. L.; Lynch, G. C.; Truhlar, D. G.; Schwenke, D. W. *J. Phys. Chem.* **1994**, *98*, 8000.

(35) Mielke, S. L.; Peterson, K. A.; Schwenke, D. W.; Garrett, B. C.; Truhlar, D. G.; Michael, J. V.; Su, M.-C.; Sutherland, J. W. *Phys. Rev. Lett.* **2003**, *91*, 063201.

(36) Mielke, S. L.; Schwenke, D. W.; Garrett, B. C.; Truhlar, D. G.; Peterson, K. A. Manuscript in preparation.

(37) Ballhausen, C. J.; Hansen, A. E. *Annu. Rev. Phys. Chem.* **1972**, *23*, 15. Garrett, B. C.; Truhlar, D. G. *J. Chem. Phys.* **1985**, *82*, 4543.

(38) Schrödinger, E. *Ann. D. Phys.* **1926**, *79*, 361.

(39) Pekeris, C. L. *Phys. Rev.* **1959**, *115*, 1216.

(40) Kolos, W.; Wolniewicz, L. *J. Mol. Spectrosc.* **1975**, *54*, 303.

(41) Moss, R. E. *Mol. Phys.* **1993**, *80*, 2541.

(42) Jaquet, R.; Cencek, W.; Kutzelnigg, W.; Rychlewski, J. *J. Chem. Phys.* **1998**, *108*, 2837. Tennyson, J.; Barletta, P.; Kostin, M. A.; Polyansky, O. L.; Zobov, N. F. *Spectrochim. Acta A* **2002**, *58*, 663.